INTERNATIONAL JOURNAL OF HYDROGEN ENERGY 42 (2017) 6448–6454

Available online at www.sciencedirect.com

ScienceDirect

journal homepage: www.elsevier.com/locate/he

Porous molybdenum carbide microspheres as efficient binder-free electrocatalysts for suspended hydrogen evolution reaction

Jie Chen [a,b], *Weijia Zhou* [a,c,*], *Jin Jia* [a], *Boao Wan* [a], *Jia Lu* [a], *Tanli Xiong* [a], *Qingxiao Tong* [b,**], *Shaowei Chen* [a,d]

[a] *New Energy Research Institute, School of Environment and Energy, South China University of Technology, Guangzhou Higher Education Mega Center, Guangzhou, Guangdong 510006, China*

[b] *Department of Chemistry, Shantou University, 243 Daxue Road, Shantou, Guangdong 515063, China*

[c] *Guangdong Provincial Key Laboratory of Atmospheric Environment and Pollution Control, South China University of Technology, Guangzhou Higher Education Mega Center, Guangzhou 510006, China*

[d] *Department of Chemistry and Biochemistry, University of California, 1156 High Street, Santa Cruz, CA 95064, United States*

ARTICLE INFO

Article history:
Received 4 October 2016
Received in revised form
9 December 2016
Accepted 11 December 2016
Available online 29 December 2016

Keywords:
Anion-exchange reaction
Molybdenum carbide microspheres
Binder-free electrocatalyst
Suspended hydrogen evolution reaction

ABSTRACT

Generally, the electrocatalysts are immobilized on conductive electrodes or in-situ grown on current-collecting substrates, which causes some disadvantages. For the first time, the obtained porous molybdenum carbide microspheres with diameters of 200–400 μm are employed as binder-free electrocatalysts in the novel model of suspended hydrogen evolution reaction (SHER), which possess the perfect catalytic stability and high practicability. Herein, porous molybdenum carbide microspheres synthesized by ion exchange reaction and subsequent calcining process are employed as electrocatalysts for HER, which possess a low onset potential of −79 mV vs. RHE and a low overpotential of 174 mV achieving a current density of 10 mA/cm^2 in 0.5 M H_2SO_4. This work may provide a new methodology for rational design and fabrication of reaction pattern for the electrolysis of water.

Introduction

Development of the effective technologies for clean and sustainable hydrogen energy have been attracting great attention lately. Hydrogen is hailed as a promising energy source to reduce our dependence on fossil fuels and benefit the environment by reducing the emissions of greenhouse and other toxic gases [1,2]. Toward this end, an effective and promising approach is based on the electrolysis of water for hydrogen evolution reaction (HER) [3–5]. Although platinum group electrocatalysts exhibit almost no overpotential, the scarcity

* *Corresponding author*. New Energy Research Institute, School of Environment and Energy, South China University of Technology, Guangzhou Higher Education Mega Center, Guangzhou, Guangdong 510006, China.
** *Corresponding author*.
E-mail addresses: eszhouwj@scut.edu.cn (W. Zhou), qxtong@stu.edu.cn (Q. Tong).
http://dx.doi.org/10.1016/j.ijhydene.2016.12.048
0360-3199/

and high costs severely limit its widespread applications [6,7]. Molybdenum-based compounds are an exciting family of HER catalysts, including MoS_2 [8–16], $MoSe_2$ [17,18], Mo_2C [19–26], $NiMoN_x$ [27], and MoP [28,29], which exhibit excellent HER activity and robust stability in acidic electrolytes. The molybdenum carbide received substantial interest in many researchers, due to its catalytic property similar to noble metals, such as strong hydrogen adsorption–desorption ability [30]. For instance, Lou et al. [19] reported that the hierarchical β-Mo_2C nanotubes were synthesized using MoO_3 nanorods as a self-degraded template and Mo precursor, which possessed excellent HER performance with an onset potential of −82 mV in 0.5 M H_2SO_4, and an overpotential of 172 mV to reach 10 mA cm^{-2}.

Generally, the powdered electrocatalysts are immobilized on conductive electrodes (such as glass carbon electrode) with Nafion as a binder, which causes some disadvantages. Firstly, the binders reduce the catalytic activity of electrocatalysts, especially in high-loading amount; Secondly, the electrocatalysts are easy to fall off from electrodes. The solution is that the active components are in-situ grown on current-collecting substrates or the establishment of three-dimensional electrodes to avoid in using the binders [31]. However, the disadvantage is that the electrocatalysts and electrodes are a whole, which are hardly replaced at any time after a long running with degenerative catalytic activity. Thus, it remains a great challenge to develop a high efficiency and binder-free model for HER.

Ion exchange resins are widely used in the removal of heavy metal ions in wastewater [32]. Yet, how to properly dispose of these materials containing heavy metal ions remain a great challenge [33]. Herein, we describe the preparation of porous molybdenum carbide microspheres derived from ion-exchange resin, which are employed as efficient binder-free electrocatalysts for suspended hydrogen evolution reaction (SHER). The Mo_2C microspheres were scattered into the electrolyte, which were not fixed on the working electrode. An equilibrium between the gravity (Fg) of Mo_2C microspheres and buoyancy (F_b) from absorbed H_2 bubbles on Mo_2C microspheres. Our results may offer a new methodology for the design and engineering of effective HER without any binder.

Experimental

Materials

All reagents were of analytical grade and used without further purification. 201 × 7 (717) strongly basic styrene type anion-exchange resin, sodium molybdate ($Na_2MoO_4 \cdot 2H_2O$) and 20 wt% Pt/C were obtained from Sinopharm Chemical Reagents Beijing Co.

Synthesis of molybdenum carbide microspheres

The synthetic process of porous molybdenum carbide microspheres are showed in Fig. S1. Typically, 5 g of anion-exchange resin was soaked in 20 mL of a 0.5 M of sodium molybdate aqueous solution. The mixture were stirred at room temperature for 12 h. Afterwards, the molybdenum containing resin microspheres was separated and washed by plenty of water, then dried at vacuum oven at 60 °C for 12 h. The molybdenum carbide microspheres were synthesized by calcining the as-obtained molybdenum containing resin microspheres at 900 °C for 2 h under Ar protection in a tube furnace. In addition, the components of molybdenum based microspheres were regulated by different calcination temperatures (700 °C, 800 °C, and 1000 °C) in a similar synthesis process. The molybdenum carbide powder was prepared by fine milling molybdenum carbide microspheres in an agate mortar.

Characterization

Field-emission scanning electron microscopy (FESEM, NOVA Nanosem 430, FEI) measurements were employed to characterize the morphologies of the as-prepared samples. Transmission electron microscopy (TEM) measurements were performed with a JOEL JEM 2100F microscope. Powder X-ray diffraction (XRD) patterns of the samples were recorded on a Bruker D8 Advance powder X-ray diffractometer with Cu Kα (λ = 0.15406 nm) radiation. X-ray photoelectron spectroscopy (XPS, PHI, Model X-tool) was performed to study the element composition and valence state. Raman spectra were recorded on a RENISHAW in Via instrument with an Ar laser source of 488 nm in a macroscopic configuration. The BET surface areas of samples were determined by using a Micromeritics ASAP 2010 instrument with nitrogen adsorption at 77 K and the Barrett–Joyner–Halenda (BJH) method. The crystal phase transition of microspheres and content of molybdenum carbide in microspheres were estimated by the differential thermal analyzer and thermal gravimetric (TGA/DSC1, METTLER TOLEDO) under O_2 atmosphere.

Electrochemical measurements for powder

Electrochemical measurements of HER were conducted with an electrochemical workstation (CHI 760E, CH Instruments Inc.) in a 0.5 M H_2SO_4 aqueous solution. A Hg/Hg_2Cl_2 electrode (saturated KCl) and carbon cloth (1 × 1 cm^2) were used as the reference and counter electrode, respectively. 5 mg of the catalyst powder was dispersed in 1 mL of 1:1 (v/v) water/ethanol mixed solvents, along with 50 μL of a Nafion solution, the mixed solution was sonicated for 30 min. Then, 5 μL of the above solution was dropcast onto the surface of the glassy carbon electrode (GCE, 3 mm), with a geotrimetic surface area of 0.07 cm^{-2}. The as-prepared catalyst film was dried at room temperature. Polarization curves were obtained by sweeping the potential from 0 to −0.5 V (vs. RHE) at a potential sweep rate of 2 mV/s. Accelerated stability tests were performed in 0.5 M H_2SO_4 at room temperature by potential cycling between +0.3 and −0.3 V (vs. RHE) at a sweep rate of 100 mV/s for 1000 cycles. Electrochemical impedance spectroscopy (EIS) spectra were acquired at an amplitude of 10 mV within the frequency range of 100 kHz to 0.01 Hz. The main arc in the EIS spectrum was fitted using a simplified Randles equivalent circuit, which consisted of an electronic resistance (Rs) in series with a parallel arrangement of a charge-transfer resistance (Rct) and a constant phase element (CPE), and the fitting parameters

were estimated through the application of the Levenberg–Marquardt minimization procedure. Cyclic voltammetry (CV) was used to probe the electrochemical double layer capacitance at nonfaradaic potentials as a means to estimate the effective electrode surface area. Current–time responses were monitored by chronoamperometric measurements for 10 h.

Electrochemical measurements for microspheres

The porous molybdenum carbide microspheres were used as electrocatalyst in the binder-free model of suspended hydrogen evolution reaction (SHER). Electrochemical measurements of HER activity were conducted with an electrochemical workstation (CHI 760E, CH Instruments Inc.) in a 0.5 M H_2SO_4 aqueous solution. A Hg/Hg_2Cl_2 electrode (saturated KCl) and carbon cloth (1×1 cm^2) were used as the reference and counter electrode, respectively. The inert metal Ti wafer with a diameter of 5 cm was used as working electrode at the bottom of electrolytic cell. 5 mg of molybdenum carbide microspheres was dispersed in an electrolyte of 0.5 M H_2SO_4 aqueous solution, which were physically deposited by gravity on the Ti electrode without any binder. Polarization curves were obtained by sweeping the potential from 0 to −0.5 V (vs. RHE) at a potential sweep rate of 5 mV/s. Current–time responses were monitored by chronoamperometric measurements for 10 h. Hydrogen production of the molybdenum carbide microspheres was carried out at −0.38 V (vs. RHE). The gas production rate was quantified by gas chromatographic measurements (GC-2060F, LuNan Analytical Instruments, LTD, China).

Results and discussion

The morphology and structure of the as-prepared Mo_2C microspheres were analyzed by field emission scanning electron microscope (FESEM) and high-resolution transmission emission microscope (HRTEM). The similar porous sphere structures of molybdenum-based compounds obtained at different temperatures (700 °C, 800 °C, 900 °C and 1000 °C) are showed in Fig. 1. Fig. 1a, c, e, g show that Mo_2C microspheres with the diameter of 200–400 μm possessed a rough surface. The abundant nanoparticles were uniformly distributed on the surface of Mo_2C porous microspheres (Fig. 1b, d, f, h). From Fig. 2a, we can clearly see that black Mo_2C nanoparticles were distributed in light amorphous carbon substrate. The content of carbon in microspheres is 19.3 wt% estimated by the differential thermal analyzer and thermal gravimetric (Fig. S2). From HRTEM image in Fig. 2b, the nanoparticles exhibited clearly-defined lattice fringe with spacing of 0.26 nm, consistent with the (100) of Mo_2C. In addition, the electron diffraction result suggested the single-crystal structure of a single Mo_2C particle (Inset of Fig. 2b).

The crystal phase transformation of microspheres obtained at different calcination temperatures were examined by XRD, XPS and Raman spectrum. As shown in Fig. 3a, when the microspheres were heated at 700 °C, pure molybdenum dioxide (MoO_2) appeared with characteristic peaks located at 26.0°, 37.1°, 53.5°, and 60.5° corresponding to (110), (101), (211) and (310) crystal faces (JCPDS file no. 02-0422). When the calcination temperature reached to 800 °C, the main phase of MoO_2 and a small quantity of Mo_2C were observed. When the temperature was increased to 900 °C and 1000 °C, the characteristic peaks at 34.4° (100), 38.0° (002), 39.4° (101), 52.1° (102), and 61.5° (110) of Mo_2C were observed (JCPDS file no. 35-0787), suggesting the pure Mo_2C can be synthesized at 900 °C or higher temperatures. The phase transformation between MoO_2 and Mo_2C was also confirmed by XPS (Fig. 3b) and Raman spectra (Fig. S3). As shown in Fig. 3b, the valence state changed from Mo^{4+} to Mo^{2+}, and the corresponding peak positions at 232.2 eV (229.2 eV) and 231.4 eV (228 eV) were observed, respectively [34]. However, a small amount of Mo^{4+} was also observed in XPS spectrum of Mo_2C-900, which was not detected by XRD due to the trace amount. In addition, Mo^{6+} with characteristic peak at 235.4 eV was detected in all samples because that the surface of Mo_2C can be readily contaminated with molybdenum oxides when exposed to air [22,35].

The specific surface area and pore size distribution of the as-obtained microspheres were then quantified by nitrogen adsorption/desorption studies. From Fig. 3c, it can be seen that all samples exhibited type IV nitrogen adsorption/desorption isotherms with a clear H_2-type hysteresis loop. Among the series, MoO_2-700 sample (synthesized at 700 °C) possessed the lowest BET surface area of 42.8 m^2/g, due to an insufficient carbonization of the resin spheres. Yet, the highest value of 136.46 m^2/g for Mo_2C-900 was obtained, then decreased to 89.75 m^2/g for Mo_2C-1000, possibly due to the collapse of the porous structure. Furthermore, the Mo_2C-900 and Mo_2C-1000 exhibited rather broad pore size distributions of 2–18 nm and 0–12 nm, with the main pore sizes of 12 nm and 7.5 nm, respectively (Fig. 3d).

To research intrinsic catalytic activity for HER, the microspheres were finely milled to powder (the morphologies as shown in Fig. S4) and loaded onto the GCE, then examined by a three-electrode system in 0.5 M H_2SO_4. Fig. 4a shows that the electrocatalytic performance of as-prepared catalysts were gradually increased with the following order of MoO_2-700, MoO_2/Mo_2C-800, Mo_2C-1000 and Mo_2C-900, corresponding onset potentials (vs. RHE) were −204 mV, −144 mV, −116 mV, and −79 mV, respectively (Fig. S5, the onset potential was determined at the current density of −0.5 mA cm^{-2}). The Mo_2C-900 as electrocatalyst possessed the best HER performance with onset potential of only −79 mV (vs. RHE) and an overpotential of 174 mV at a current density of 10 mA cm^{-2}. However, the HER activity of Mo_2C was worse than that of 20 wt% Pt/C (−3 mV vs. RHE). Fig. 4b shows that the corresponding Tafel plots of as-prepared products. A Tafel slope of 73.32 mV/dec showed that the HER for Mo_2C-900 proceeded through a Volmer–Heyrovsky mechanism [36] and the electrochemical desorption process was the rate-limiting step. The value is much lower than those of MoO_2-700 (153.37 mV/dec) and MoO_2/Mo_2C-800 (128.59 mV/dec), but slightly larger than that of Mo_2C-1000 (63.99 mV/dec), which implied that the higher annealing temperatures can promote the electrochemical desorption reaction. In addition, the Mo_2C-900 also possessed an exchange current density of 0.050 mA cm^{-2} larger than MoO_2-700 (0.018 mA cm^{-2}), MoO_2/Mo_2C-800 (0.04 mA cm^{-2}) and

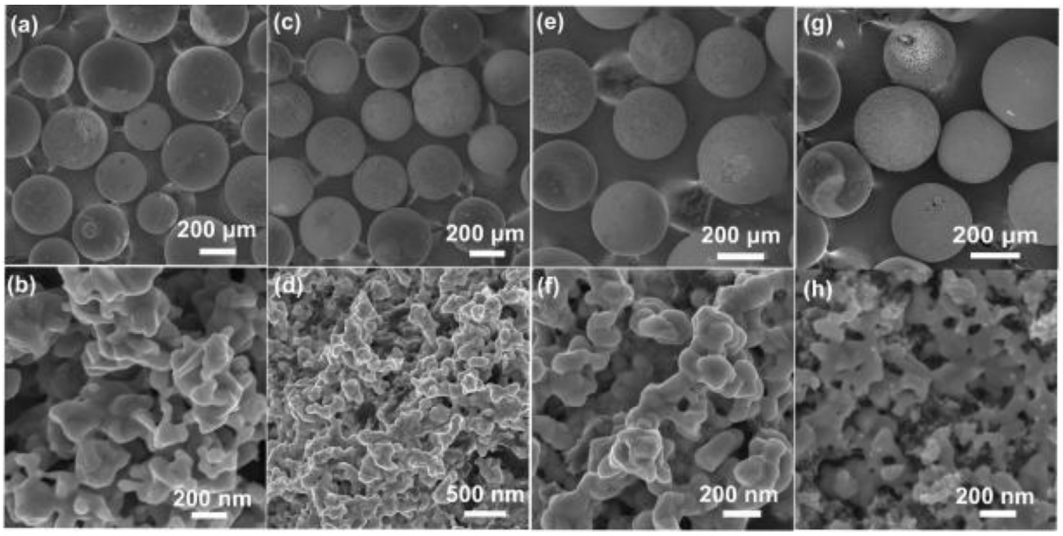

Fig. 1 – (a) SEM images of microspheres synthesized by different temperatures: (a, b) 700 °C, (c, d) 800 °C, (e, f) 900 °C and (g, h) 1000 °C.

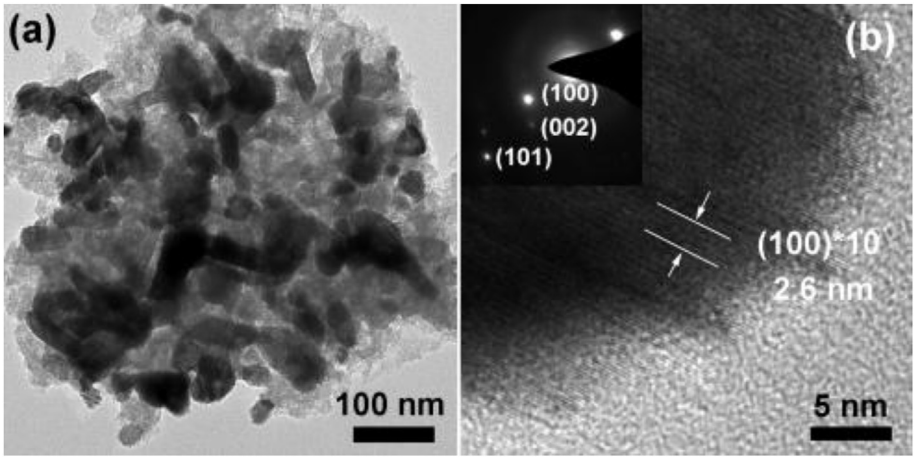

Fig. 2 – (HR)TEM images of Mo_2C synthesized at 900 °C. Inset is the selected area electron diffraction patterns (The zone axis of the pattern is <200>).

Mo_2C-1000 (0.003 mA cm^{-2}) (Fig. S6). The typical Nyquist plots of the EIS response of all samples at a applied potential of 150 mV are showed in Fig. S7a, the Rs (the series resistance) value of MoO_3-700, MoO_3/Mo_2C-800, Mo_2C-900, Mo_2C-1000 were obtained and then used to correct the polarization curves (Fig. S8). Mo_2C-modified electrodes at various overpotentials showed that the diameter of the semicircles decreased apparently with the increase of overpotentials, from 892.4 Ω at 100 mV to 168 Ω at 200 mV, suggesting decreasing charge-transfer resistance (Rct) with increasingly negative electrode potentials (Fig. S7b).

Cyclic voltammograms were employed to estimate the electrochemically active surface area. The CVs of samples synthesized by the different temperatures are showed in Fig. S9, and corresponding capacitances of 5.2 mF/cm^2 (MoO_2-700), 6.7 mF/cm^2 (MoO_2/Mo_2C-800), 23.1 mF/cm^2 (Mo_2C-1000) and 57.57 mF/cm^2 (Mo_2C-900) are showed in Fig. 4c. However, after being corrected by electrochemical area, Mo_2C-900 still possessed the smallest onset potential (Fig. S10), implying that electrochemical area can only affect the catalytic current density, rather than the intrinsic catalytic activity.

The catalytic stability measured by accelerated degradation testing and chronopotentiometry is the crucial aspect for HER. The polarization curves of Mo_2C-900 before and after 1000 cycles confirmed the good stability with a slight decrease of current density (Inset of Fig. 4d). At an overpotential of 300 mV, the Mo_2C-900-modified electrode was operated continuously for 10 h and a small loss of current density (8.3%) was observed, suggesting the long-term extraordinary durability for HER in 0.5 M H_2SO_4 (Fig. 4d). It's worth noting that HER performance of Mo_2C-900 was equivalent or better than the leading molybdenum-based catalysts, which are summarized in Table S1.

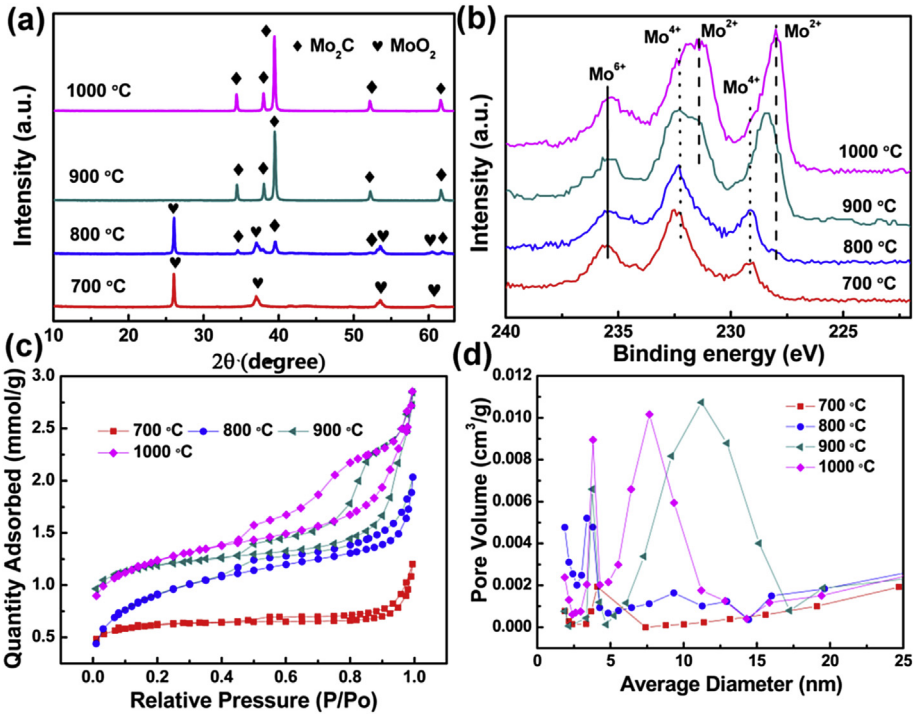

Fig. 3 – (a) XRD patterns, (b) X-ray photoelectron spectra of Mo 3d, (c) Nitrogen adsorption/desorption isotherms and (d) pore size distributions of microspheres synthesized by different temperatures (700 °C, 800 °C, 900 °C and 1000 °C).

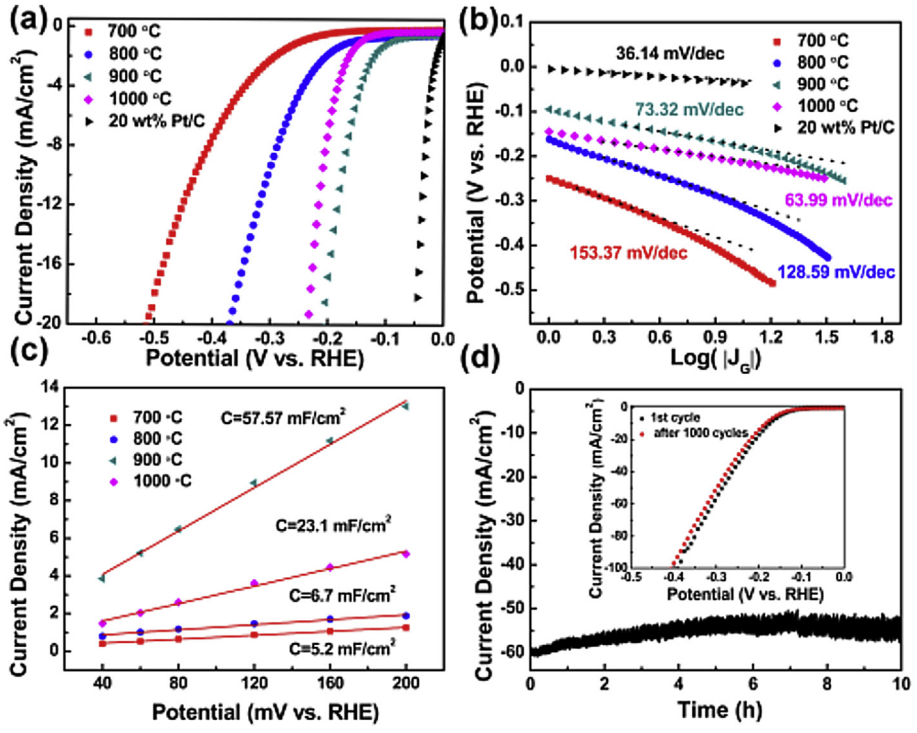

Fig. 4 – (a) Polarization curves (IR-uncorrected) of the samples synthesized at different annealing temperatures (700 °C, 800 °C, 900 °C and 1000 °C) in 0.5 M H_2SO_4 at a scan rate of 2 mV s^{-1} and (b) Corresponding Tafel plots of as-prepared products. (c) Plots of capacitive current as a function of scan rate for the obtained samples. (d) Current–time plots of Mo_2C-900 with the overpotential of 300 mV. The inset is polarization curves before and after 1000 potential cycles in the stability tests.

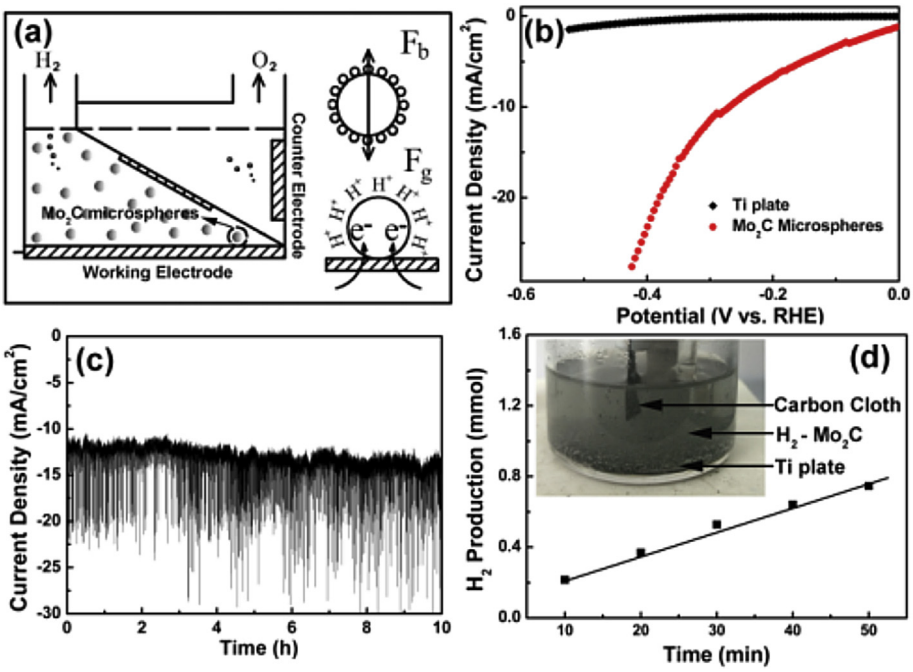

Fig. 5 – (a) The schematic diagram of SHER, (b) Polarization curves of Mo_2C microspheres on Ti plate in 0.5 M H_2SO_4 at a scan rate of 5 mV s^{-1}. Current–time plots (c) and hydrogen production (d) of SHER at −300 mV vs. RHE. Inset is the digital photo of SHER.

The schematic diagram of SHER are showed in Fig. 5a. The different pattern was that the Ti plate as inert working electrode was placed at the bottom of electrolytic cell. The Mo_2C microspheres were scattered into the electrolyte, which were not fixed on the working electrode by binder. When the Mo_2C microspheres deposited on the bottom of electrolytic cell by gravity (F_g), the electrons transported from the cathode to Mo_2C microspheres. After that, the H_2 gas was accompanied on the surface of Mo_2C microspheres. When the enough buoyancy (F_b) from absorbed H_2 bubbles equal to F_g (the gravity of Mo_2C microspheres), Mo_2C microspheres suspended in the electrolyte. The H_2/Mo_2C microspheres collided with each other in the electrolyte to remove H_2 bubbles from the surface of Mo_2C microspheres. Then, the Mo_2C microspheres sinked onto the inert Ti plate. The above-mentioned three processes formed a loop for SHER. The polarization curves of Ti plate (no activity for HER) and Mo_2C microspheres are showed in Fig. 5b, and the overpotential for Mo_2C microspheres was 248 mV to achieve a current density of 10 mA cm^{-2}. Fig. 5c shows the corresponding current–time plots of Mo_2C microspheres at −300 mV vs. RHE, which showed an excellent HER stability for 10 h. It's worth noting that the current density of SHER slightly increased with the long running time (128%), which was much better than that loaded on GCE for HER (91.7%). A digital photo of SHER is shown in the inset of Fig. 5d. The gathered bubbles were hydrogen, which were confirmed by gas chromatography, and the corresponding hydrogen production rate was 40.22 mmol g^{-1} h^{-1}. One thing we should focus on is that Mo_2C microspheres are easy to be recycled and replaced in electrolytic cell (Fig. S11), and it is the distinct advantage of SHER.

Conclusion

In this study, the obtained porous Mo_2C microspheres with diameters of 200–400 μm were employed as binder-free electrocatalysts in the novel model of SHER, which was driven by the equilibrium between the gravity (F_g) of Mo_2C microspheres and buoyancy (F_b) from absorbed H_2 bubbles on Mo_2C microspheres. Porous Mo_2C powder with the large surface area of 136.46 m^2/g offered abundant active sites for HER, and the ultrathin carbon in Mo_2C promoted the electron transport, it all caused the excellent HER performance for water splitting. A new running way of SHER (without any binder) possessed the perfect catalytic stability and high practicability, which provided a new catalytic way for catalyzing water splitting.

Acknowledgements

This work was supported by Project of Public Interest Research and Capacity Building of Guangdong Province (2014A010106005), the National Natural Science Foundation of China (51502096, 51273108), Guangdong Innovative and Entepreneurial Research Team Program (2014ZT05N200) and the National Basic Research Program of China (2013CB834803).

Appendix A. Supplementary data

Supplementary data related to this article can be found at http://dx.doi.org/10.1016/j.ijhydene.2016.12.048.

REFERENCES

[1] Dresselhaus M, Thomas I. Alternative energy technologies. Nature 2001;414:332–7.
[2] Turner JA. Sustainable hydrogen production. Science 2004;305:972–4.
[3] Jiao Y, Zheng Y, Jaroniec M, Qiao SZ. Design of electrocatalysts for oxygen- and hydrogen-involving energy conversion reactions. Chem Soc Rev 2015;44:2060–86.
[4] Zhou W, Xiong T, Shi C, Zhou J, Zhou K, Zhu N, et al. Bioreduction of precious metals by microorganism: efficient Gold@N-doped carbon electrocatalysts for the hydrogen evolution reaction. Angew Chem Int Ed 2016;128:8556–60.
[5] Subbaraman R, Tripkovic D, Strmcnik D, Chang K-C, Uchimura M, Paulikas AP, et al. Enhancing hydrogen evolution activity in water splitting by tailoring Li^+-$Ni(OH)_2$-Pt interfaces. Science 2011;334:1256–60.
[6] Walter MG, Warren EL, McKone JR, Boettcher SW, Mi Q, Santori EA, et al. Solar water splitting cells. Chem Rev 2010;110:6446–73.
[7] Gray HB. Powering the planet with solar fuel. Nat Chem 2009;1. 7–7.
[8] Yang L, Zhou W, Hou D, Zhou K, Li G, Tang Z, et al. Porous metallic MoO_2-supported MoS_2 nanosheets for enhanced electrocatalytic activity in the hydrogen evolution reaction. Nanoscale 2015;7:5203–8.
[9] Gopalakrishnan D, Damien D, Shaijumon MM. MoS_2 quantum dot-interspersed exfoliated MoS_2 nanosheets. ACS Nano 2014;8:5297–303.
[10] Lu Z, Zhu W, Yu X, Zhang H, Li Y, Sun X, et al. Ultrahigh hydrogen evolution performance of under-water "Superaerophobic" MoS_2 nanostructured electrodes. Adv Mater 2014;26:2683–7.
[11] Yu Y, Huang S-Y, Li Y, Steinmann SN, Yang W, Cao L. Layer-dependent electrocatalysis of MoS_2 for hydrogen evolution. Nano Lett 2014;14:553–8.
[12] Kibsgaard J, Chen Z, Reinecke BN, Jaramillo TF. Engineering the surface structure of MoS_2 to preferentially expose active edge sites for electrocatalysis. Nat Mater 2012;11:963–9.
[13] Liao L, Zhu J, Bian X, Zhu L, Scanlon MD, Girault HH, et al. MoS_2 formed on mesoporous graphene as a highly active catalyst for hydrogen evolution. Adv Funct Mater 2013;23:5326–33.
[14] Wang T, Liu L, Zhu Z, Papakonstantinou P, Hu J, Liu H, et al. Enhanced electrocatalytic activity for hydrogen evolution reaction from self-assembled monodispersed molybdenum sulfide nanoparticles on an Au electrode. Energy Environ Sci 2013;6:625–33.
[15] Voiry D, Salehi M, Silva R, Fujita T, Chen M, Asefa T, et al. Conducting MoS_2 nanosheets as catalysts for hydrogen evolution reaction. Nano Lett 2013;13:6222–7.
[16] Yang L, Zhou W, Lu J, Hou D, Ke Y, Li G, et al. Hierarchical spheres constructed by defect-rich MoS_2/carbon nanosheets for efficient electrocatalytic hydrogen evolution. Nano Energy 2016;22:490–8.
[17] Tang H, Dou K, Kaun C-C, Kuang Q, Yang S. $MoSe_2$ nanosheets and their graphene hybrids: synthesis, characterization and hydrogen evolution reaction studies. J Mater Chem A 2014;2:360–4.
[18] Saadi FH, Carim AI, Velazquez JM, Baricuatro JH, McCrory CC, Soriaga MP, et al. Synthesis of macroporous molybdenum diselenide films for electrocatalysis of the hydrogen-evolution reaction. ACS Catal 2014;4:2866–73.
[19] Ma FX, Wu HB, Xia BY, Xu CY, Lou XWD. Hierarchical β-Mo_2C nanotubes organized by ultrathin nanosheets as a highly efficient electrocatalyst for hydrogen production. Angew Chem Int Ed 2015;54:15395–9.
[20] Wu HB, Xia BY, Yu L, Yu X-Y, Lou XWD. Porous molybdenum carbide nano-octahedrons synthesized via confined carburization in metal-organic frameworks for efficient hydrogen production. Nat Commun 2015;6:6512.
[21] Liao L, Wang S, Xiao J, Bian X, Zhang Y, Scanlon MD, et al. A nanoporous molybdenum carbide nanowire as an electrocatalyst for hydrogen evolution reaction. Energy Environ Sci 2014;7:387–92.
[22] Xiao P, Yan Y, Ge X, Liu Z, Wang J-Y, Wang X. Investigation of molybdenum carbide nano-rod as an efficient and durable electrocatalyst for hydrogen evolution in acidic and alkaline media. Appl Catal B Environ 2014;154:232–7.
[23] Ge C, Jiang P, Cui W, Pu Z, Xing Z, Asiri AM, et al. Shape-controllable synthesis of Mo_2C nanostructures as hydrogen evolution reaction electrocatalysts with high activity. Electrochim Acta 2014;134:182–6.
[24] Chen W-F, Wang C-H, Sasaki K, Marinkovic N, Xu W, Muckerman J, et al. Highly active and durable nanostructured molybdenum carbide electrocatalysts for hydrogen production. Energy Environ Sci 2013;6:943–51.
[25] Zhong Z, Liu N, Chen H, Fu X, Yang L, Gao Q. Molybdenum carbide supported by N-doped carbon: controlled synthesis and application in electrocatalytic hydrogen evolution reaction. Mater Lett 2016;176:101–5.
[26] Tuomi S, Guil-Lopez R, Kallio T. Molybdenum carbide nanoparticles as a catalyst for the hydrogen evolution reaction and the effect of pH. J Catal 2016;334:102–9.
[27] Chen WF, Sasaki K, Ma C, Frenkel AI, Marinkovic N, Muckerman JT, et al. Hydrogen-evolution catalysts based on non-noble metal nickel-molybdenum nitride nanosheets. Angew Chem Int Ed 2012;51:6131–5.
[28] Xiao P, Sk MA, Thia L, Ge X, Lim RJ, Wang J-Y, et al. Molybdenum phosphide as an efficient electrocatalyst for the hydrogen evolution reaction. Energy Environ Sci 2014;7:2624–9.
[29] McEnaney JM, Crompton JC, Callejas JF, Popczun EJ, Biacchi AJ, Lewis NS, et al. Amorphous molybdenum phosphide nanoparticles for electrocatalytic hydrogen evolution. Chem Mater 2014;26:4826–31.
[30] Sheng W, Zhuang Z, Gao M, Zheng J, Chen JG, Yan Y. Correlating hydrogen oxidation and evolution activity on platinum at different pH with measured hydrogen binding energy. Nat Commun 2015;6:5848.
[31] Zhou W, Zhou Y, Yang L, Huang J, Ke Y, Zhou K, et al. N-doped carbon-coated cobalt nanorod arrays supported on a titanium mesh as highly active electrocatalysts for the hydrogen evolution reaction. J Mater Chem A 2015;3:1915–9.
[32] Mahmoud A, Hoadley AFA. An evaluation of a hybrid ion exchange electrodialysis process in the recovery of heavy metals from simulated dilute industrial wastewater. Water Res 2012;46:3364–76.
[33] Zhou Y, Zhou W, Hou D, Li G, Wan J, Feng C, et al. Metal–carbon hybrid electrocatalysts derived from ion-exchange resin containing heavy metals for efficient hydrogen evolution reaction. Small 2016;12:2768–74.
[34] Zhou W, Hou D, Sang Y, Yao S, Zhou J, Li G, et al. MoO_2 nanobelt@nitrogen self-doped MoS_2 nanosheets as effective electrocatalysts for hydrogen evolution reaction. J Mater Chem A 2014;2:11358–64.
[35] Xiang M, Li D, Li W, Zhong B, Sun Y. Potassium and nickel doped β-Mo_2C catalysts for mixed alcohols synthesis via syngas. Catal Commun 2007;8:513–8.
[36] Morales-Guio CG, Stern L-A, Hu X. Nanostructured hydrotreating catalysts for electrochemical hydrogen evolution. Chem Soc Rev 2014;43:6555–69.